# Efficiency and Reliability of Gravity Die Casting Models for Simulation Based Design

A. Vergnano[1,2(✉)], E. Brambilla[1], and G. Bonfiglioli[1]

[1] Modelleria Brambilla S.p.a., Via del progresso 1, 42015 Correggio, RE, Italy
alberto.vergnano@unimore.it
[2] Department of Engineering "Enzo Ferrari", University of Modena and Reggio Emilia, Via Pietro Vivarelli 10, 41125 Modena, Italy

**Abstract.** Simulation of Gravity Die Casting (GDC) requires coupling different models for fluid dynamics, heat transfer and solidification, together with material physics properties. Very long calculation times are required since several heating and production cycles have to be run. The simplification of the simulation models is critical to have results in times suitable for the design process. The present work discusses the solidification and heat transfer physics with simplification hypotheses. A simulation approach skipping the pouring model for the heating cycles is introduced. A realistic case study on an engine head GDC is presented to evaluate four possible simulation sequences. The results show that including the heating cycles in the simulation is advisable. The simplified sequences reproduce the temperature field of the die with sufficient accuracy. The proposed simulation approach results in considerable time saving with respect to the actual simulations and even in accuracy improvements.

**Keywords:** Gravity die casting · Process simulation · Model efficiency · Model reliability · Simulation based design

## 1 Introduction

Gravity Die Casting (GDC) is an ancient but extremely complex technology, the output quality resulting from the interaction of very many mechanics, physics and chemistry factors [1]. The present research investigates dies for casting of aluminum engine parts, namely engine heads, cylinder blocks and crankcases. Each die is a one-off design but conceived to deliver more than 100,000 quality castings as operating life specification. Moreover, it is very expensive and must be designed, manufactured and delivered to foundries in few months.

A design engineer must conceive the die as a thermal machine. The casting shape determines the die layout and slides, while the pattern size must be scaled to account for thermal expansion of die steel, contraction of solidifying alloy and negligible variation of cores. Moreover, differential heat removal should provide a directional and fast solidification in order to avoid porosities and deliver good material properties regarding Secondary Dendrite Arm Spacing (SDAS) [2].

Nowadays, simulation is a fundamental design tool to handle so many factors [3–5]. However, the models for casting simulations are computationally heavy, since


F. Cavas-Martínez et al. (Eds.): *Advances on Mechanics, Design Engineering and Manufacturing II*, LNME, pp. 3–12, 2019.
https://doi.org/10.1007/978-3-030-12346-8_1

they involve coupled fluid dynamics, heat transfer and metallurgy phenomena equations [6–9]. Moreover, several heating and production cycles must be simulated to reproduce the actual warmed up equipment. In the current design practice, such simulations can require 2 or 3 days run on a workstation with 8 parallel cores and 64 GB RAM. Those long run times make the simulations unsuitable for virtual concepts in the early design stages [10], thus they are used for the final adjustments with a limited number of trials.

The present research focuses on possible simplifications of a GDC process model in order to reduce the simulation run time, improving its role in the decision-making process [11]. Anglada et al. discussed possible simplifications of High Pressure Die Casting (HPDC) simulation [12]. The solidification model usually runs much faster than the pouring one. Considering HPDC, a sequence of heating cycles skipping the pouring model, thus running only the solidification one, is capable to reproduce the temperature field on the actual die. The pouring model is clearly critical in HPDC for cavity filling and air entrapment. On the other hand, GDC involves quite different cycle times. As a rule of thumb, the velocities at the casting gates can be about 0.3–0.5 m/s for GDC and 25–70 m/s for HPDC. HPDC is characterized also by higher heat removal rates, since thinner coating is used and high pressure up to 1200 bar is applied [13].

The pouring model in GDC determines the non-uniform temperature field of the solidifying alloy. The solidification dynamics is critical for GDC, but it is very conditioned by such initial temperature field [14]. On the other hand, the two models must run coupled, since solidification often starts when the pouring phase must still finish. The different involved phenomena require a specific investigation on GDC to determine if the heating cycles can be limited to solidification models or not.

The paper is organized as follows: Sect. 2 introduces the casting model and discusses some solidification physics, especially looking at the heat removal during alloy solidification, Sect. 3 introduces some hypotheses and four possible simulation approaches, compared with a realistic case study, Sect. 4 finally discusses the simulation results, whereas Sect. 5 draws the concluding remarks.

## 2 Gravity Die Casting Model

A GDC cycle can be modeled including the phases of die preparation, melt alloy pouring, solidification and cooling after eject, as shown in Fig. 1. This section discusses solidification and heat transfer phenomena to explain the hypotheses of the following methodology.

Metal alloys solidify over the range between Liquidus $T_{LIQ}$ and Solidus $T_{SOL}$ temperatures. So, a solidification model must consider a pseudo specific heat of the liquid, solid or two phases solution as function of temperature $T$ as

$$c^* = \begin{cases} c_{SOL}; & T < T_{SOL} \\ f_{SOL}c_{SOL} + (1 - f_{SOL}) \cdot c_{LIQ} - L_F \cdot \partial f_{SOL}/\partial T; & T_{SOL} \le T \le T_{LIQ} \\ c_{LIQ}; & T > T_{LIQ} \end{cases} \quad (1)$$

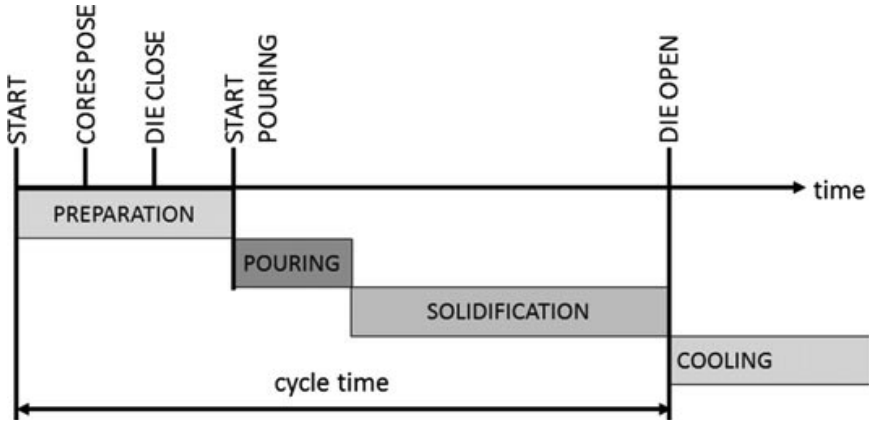


**Fig. 1.** Phases sequence in a GDC cycle

where $c_{SOL}$ and $c_{LIQ}$ are the specific heats of the solid and liquid phases respectively, $f_{SOL}$ is the solid fraction and $L_F$ is the latent heat of fusion [15, 16]. A qualitative pseudo specific heat relationship on temperature is shown in Fig. 2.

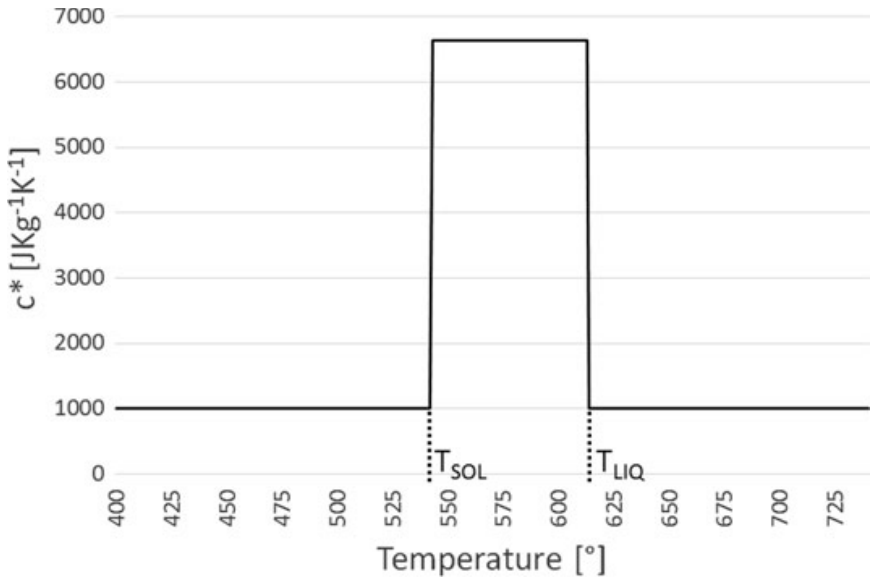


**Fig. 2.** Qualitative pseudo specific heat for an Al alloy

The heat supplied by a casting element to the adjacent die one is

$$q = \int_{T_I}^{T_F} \text{c*dT} \tag{2}$$

where the initial $T_I$ and final $T_F$ temperatures vary for different casting elements.

The heat transfer between casting and die is difficult to determine, depending on contact pressure, surface finishing, coating thickness and deformation of casting. Those factors can be modeled together as Heat Transfer Coefficient (HTC) between contact

surfaces. The HTCs are identified with experimental and inverse optimization procedures [17, 18]. Many factors depend on set up conditions and can be considered constant. However, the casting shrinkage for progressive solidification and cooling may occur in an air gap, determining a drop of the HTC from $T_{LIQ}$ to $T_{SOL}$ [18, 19]. A qualitative temperature dependent HTC is shown in Fig. 3.

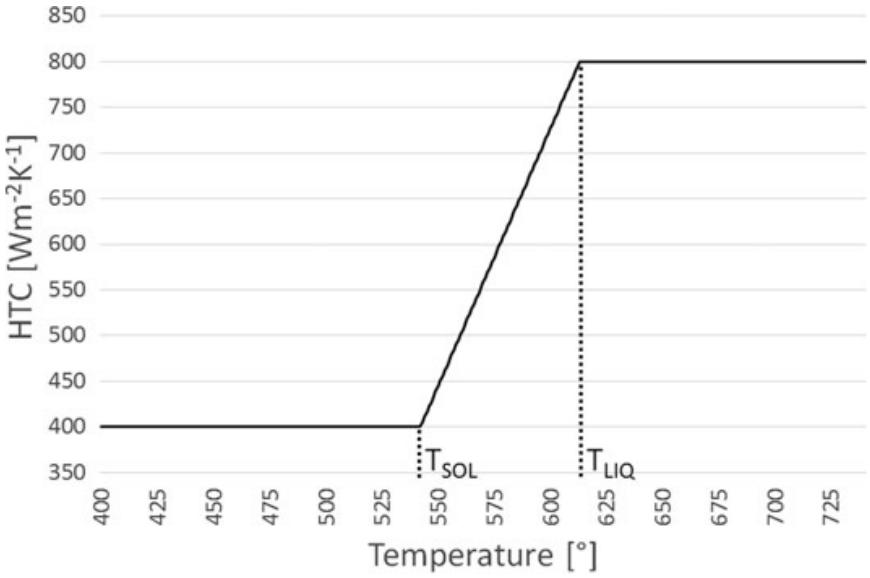


**Fig. 3.** Qualitative temperature dependent HTC

## 3 Methodology

### 3.1 Considerations on Simplification

In a DGC model the alloy is poured at uniform temperature $T_P$ and cools down while flowing into the cavities. The alloy fills each element at a $T_I$ higher, or at most little lower, than $T_{LIQ}$. Then it continues heating the die till the end of this pouring phase. In the already filled elements the temperature continues decreasing, generally still above $T_{LIQ}$ but even much below $T_{LIQ}$ in some cases. The solidification phase starts from a temperature $T_S < T_I$ as delivered by the pouring simulation and ends at $T_F$ when the die is opened. From (2), $q_P$ is the heat provided in the pouring phase, when cooling from $T_I$ to $T_S$, while $q_S$ is provided in the solidification phase, when cooling from $T_S$ to $T_F$.

In the current practice, a sequence of 4–14 heating cycles is sufficient for reproducing the non-uniform temperature field of the warmed-up die. The last production cycle delivers the results the designer is interested in. The die temperature is adjusted at each *i*th cycle and the temperatures $T_{I,i}$, $T_{S,i}$ and $T_{F,i}$ vary as a consequence. However, the pouring phase is skipped for most heating cycles to save a lot of time. It is calculated just for few ones in order to improve the simulation accuracy. If a pouring phase is not calculated in the *i*th cycle, the sequent solidification phase starts from $T_{S,i-1}$ as calculated in the previous $(i–1)th$ cycle. Thus, the temperature decrease from $T_P$ to $T_{S,i-1}$ is not considered and $q_{P,i-1}$ is lost for the simplified cycles. Referring to (2) and to Fig. 2, $q_{P,i-1}$ is a negligible amount if $T_{S,i-1} > T_{LIQ}$. However, for the casting elements

with $T_{S,i-1} < T_{LIQ}$, part of the contribution of $-L_F \cdot \partial f_S / \partial T$ of (1) is not considered, which is much more important than $(1-f_{SOL})c_{LIQ}$. So, a cycle skipping the pouring model, thus running only the solidification one, may underestimate the die heating. The temperature dependent HTC even worsen the error. The same $T_S < T_{LIQ}$, thus in the sloped curve of Fig. 3, determines a much lower HTC and limits the transfer of the already reduced available heat.

### 3.2 Simulation Approaches

The heating cycles must be simplified in order to compute results in times useful for the industry design process [14]. The solidification phase is calculated in all heating and production cycles. Four simulation approaches with calculation or not of pouring in the heating cycles are designed in order to evaluate the hypotheses:

- *H*1-7/*P*8: all the 7 heating and the final 8th production cycles are calculated;
- *P*1: only 1 production cycle is calculated, avoiding heating;
- *H*1/*P*8: calculation of the 1st and 8th cycles only;
- *H*-/*P*8: calculation of pouring for the 8th cycle only, after 7 heating ones.

The calculation of all phases in all cycles, *H*1-7/*P*8, is assumed as reference for the accuracy with the actual foundry process. It is not feasible in a design process due to the excessive computation times. *P*1 is the simplified approach currently used in the early design phases. The maximum error for the approach *P*1 is considered the 100% possible error for the following evaluations. *H*1/*P*8 is the approach currently used in the detailed design phases for the final adjustments and it is assumed as reference for the simulation time in the evaluations. From 2nd to 7th cycles $T_{S,i}$ is assumed equal to $T_{S,1}$. *H*-/*P*8 is the suggested approach to keep the results reliability of *H*1-7/*P*8 and *H*1/*P*8 while trying to reduce the computation time as *P*1. With this approach, from 1st to 7th cycles $T_{S,i}$ is assumed constant and equal to $T_P$.

### 3.3 Case Study

This paper reports a case study on GDC for an engine head with Magma 5.3.1 software [20]. It was not possible to use an existing CAD model, due to non disclosure agreement with car manufacturers. So, an engine head has been especially modeled for evaluating the previous four approaches. However, it is representative of all the features of actual dies, as cycle timing, geometries, materials, overall masses, top feeders, all cores, die parts, surface coating and thermocouples, as shown in Fig. 4.

Also, cooling channels are provided from the combustion chambers for delivering good material SDAS. The die is conceived to be operated on a tilting machine. The model of the GDC cycle consists of these phases:

1. preparation: 45 s for cleaning, cores pose, die close, die tilting back in the −90° position;
2. pouring: instantaneous pouring cup filling, then 15 s for tilting from −90° to 0°;
3. solidification: 255 s waiting in 0° position, then die open;
4. casting ejection, external cooling.

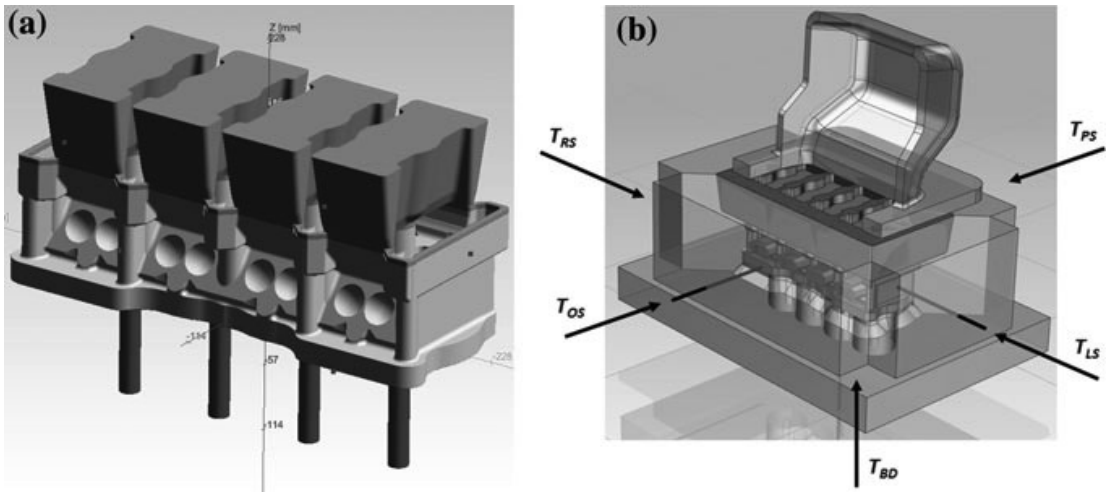


**Fig. 4.** CAD assemblies of **a** engine head casting, feeder, cooling channels and **b** pouring cup, die parts, cores, thermocouples $T_{BD}$, $T_{OS}$, $T_{PS}$, $T_{LS}$, $T_{RS}$

These materials are modeled: AlSi7Mg alloy poured at $T_P$ = 740 °C in the pouring cup, X38CrMoV5 steel for the die at 250 °C initial constant temperature, silica sand for cores at 40 °C initial constant temperature. The AlSi7Mg alloy is characterized by $T_{SOL}$ = 542 °C and $T_{LIQ}$ = 613 °C. The die temperatures are monitored with 5 thermocouples into the die: $T_{BD}$ in the bottom die, $T_{OS}$ and $T_{PS}$ in the opposite and pouring slides, while $T_{LS}$ and $T_{RS}$ in the left and right sides. In order to reduce the computation time, the mesh is quite rough, with only 118,295 cavity cells. Please consider that the actual models are much heavier, with 2,000,000 cells or more. Figure 5 shows the temperature results for the pouring simulation of the 8th cycle at three time-steps. The temperature field is not constant and the next solidification phase will start from a temperature $T_{S,8} < T_{I,8} < T_P$. Moreover, $T_{S,8} < T_{LIQ}$ in some elements.

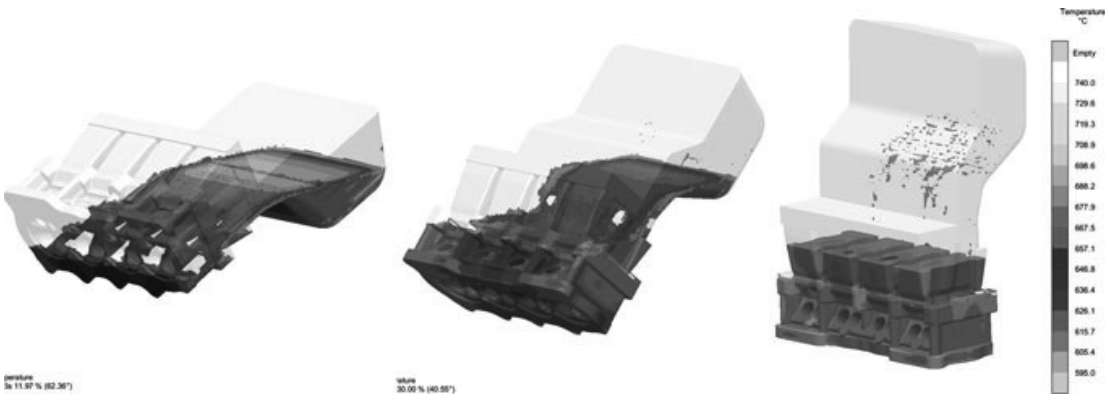

**Fig. 5.** Temperature results during the pouring phase at 4.6 s, 8.2 s and 15.0 s

## 4 Results and Discussion

The computation times needed for the different simulation approaches are reported in Table 1. These times have been obtained on a workstation with 8 parallel cores and 64 GB RAM. The complete simulation *H*1-7/*P*8 would increase the computation time by +207%. *P*1 would reduce it by −53%. The suggested approach *H*-/*P*8 would save −35% time.

**Table 1.** Computation times for different simulation approaches

| *H*1-7/*P*8 | *P*1 | *H*1/*P*8 | *H*-/*P*8 |
|---|---|---|---|
| 3 h 4 m/307% | 0 h 28 m/47% | 1 h 0 m/100% | 39 m/65% |

The evolution of the temperatures for all the 8 cycles is reported in Fig. 6 for *H*1-7/*P*8. It can be observed that not including the heating cycles would very reduce the results effectiveness. Clearly, this drawback can be reduced by setting a different initial temperature to each die part, recurring to previous simulations. However, this temperature would be constant from die surface to its internal material. A non-constant temperature field, higher on surface and lower in depth, would be fundamental to reproduce the heat transfer through the HTCs and the heat capacity of the massive steel.

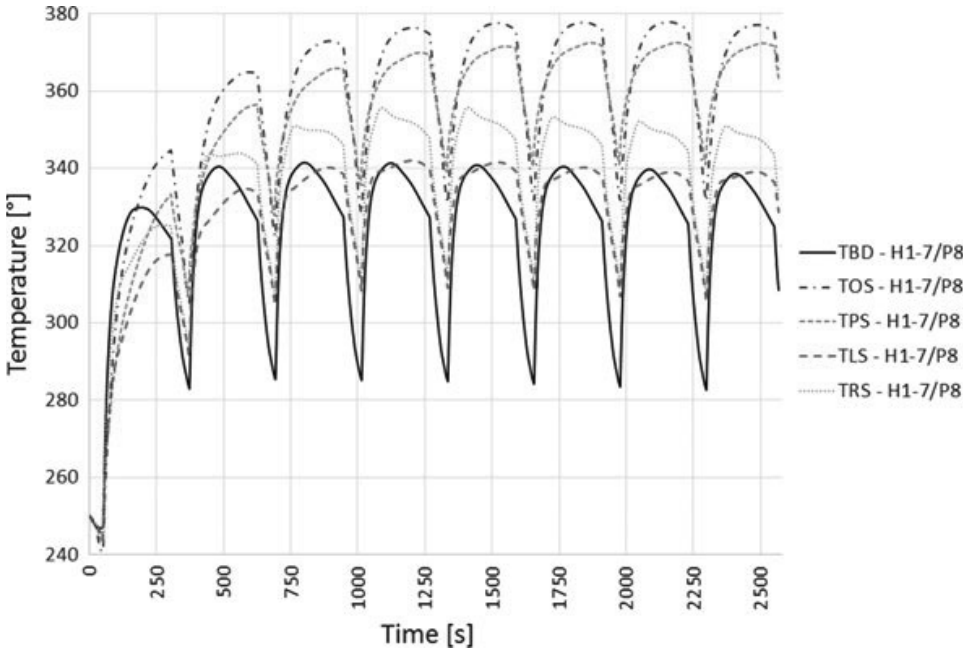


**Fig. 6.** Evolution of temperatures for the eight cycles in the H1-7/P8 approach, as sampled by the simulated thermocouples $T_{BD}$, $T_{OS}$, $T_{PS}$, $T_{LS}$, $T_{RS}$

The evolution of the temperature for the last production cycle is reported in Fig. 7 for all four approaches and five thermocouples. The solid curves describe the reference *H*1-7/*P*8 approach. As expected, *P*1 delivers results too conditioned by the initial temperature. *H*1/*P*8 underestimates die heating in all five thermocouples. *H*-/*P*8

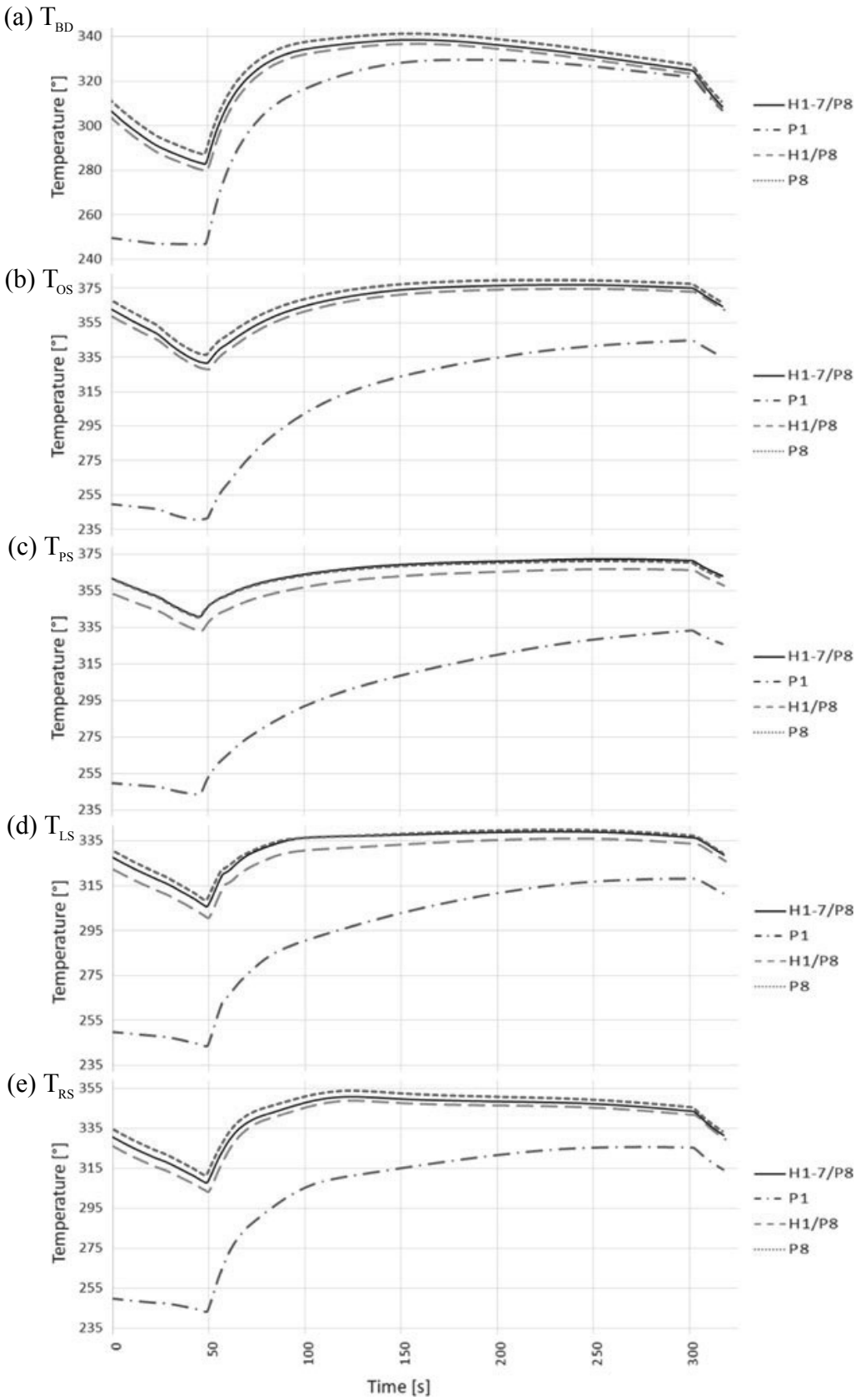


**Fig. 7.** Evolution of temperatures in the last production cycle for the simulation approaches *H*1-7*/P*8, *P*1, *H*1*/P*8, *P*8, as sampled by the thermocouples **a** $T_{BD}$, **b** $T_{OS}$, **c** $T_{PS}$, **d** $T_{LS}$, **e** $T_{RS}$

approach slightly overestimates die heating, except for $T_{PS}$, where not considering the alloy flow from the pouring cup slightly underestimates the temperature.

The temperature errors, measured at the end of the last preparation phase, just before pouring, are reported in Table 2. The final average considers the absolute value of the errors. The approach *P*1 results in a 72.0% error while *H*1/*P*8 improves the accuracy by 4.9%. *H*-/*P*8 results in a 3.3% error.

**Table 2.** Temperature errors at the end of the last preparation phase

| | *H*1-7/*P*8 | *P*1 | *H*1/*P*8 | *H*-/*P*8 |
|---|---|---|---|---|
| $T_{BD}$ | 0°/0% | −35.8°/−36.8% | −2.9°/−3.0% | 4.4°/4.5% |
| $T_{OS}$ | 0°/0% | −90.9°/−93.5% | −3.9°/−4.0% | 4.9°/5.0% |
| $T_{PS}$ | 0°/0% | −97.2°/−100% | −7.8°/−8.0% | −0.3°/−0.3% |
| $T_{LS}$ | 0°/0% | −62.0°/−63.7% | −4.8°/−4.9% | 2.9°/3.0% |
| $T_{RS}$ | 0°/0% | −64.3°/−66.1% | −4.2°/4.3% | 3.8°/3.9% |
| Average | 0°/0% | 70.0°/72.0% | 4.7°/4.9% | 3.2°/3.3% |

## 5 Conclusions

In the present paper, a discussion about the physics of aluminum alloy solidification and heat transfer to the die is presented. Four approaches for GDC simulation are defined with different simplification hypotheses. A complex model representative of real cases enables to evaluate the approaches. The complete and simplified simulations confirm the results reported in literature for HPDC [12].

The *H*1-7/*P*8 approach with no simplifications is assumed as reference for the evaluations. It can be estimated that it would require a computation time of about 6–8 days for the actual models in the industry design process, confirming its unfeasibility. The most simplified *P*1 approach is the reference for the maximum error and its simulation confirms that it leads to results too biased by the initial conditions. So, it is advisable to include the heating cycles in the simulation to reproduce the heat removal capability of the die. The simplified *H*1/*P*8 and *H*-/*P*8 approaches are both capable of reproducing the temperature field on the warmed-up die. However, the newly proposed *H*-/*P*8 presents a great reduction of computation time as −35% than *H*1/*P*8. For the proposed case study, *H*-/*P*8 shows even a slight accuracy improvement than *H*1/*P*8.

The calculation of the solidification models only is sufficient for the heating cycles, with the goal of an effective die heating. However, the cycle times for GDC are so different than HPDC that the solidification dynamics is much more influenced by the temperature field resulting from the pouring phase. The pouring simulation becomes critical in GDC for the goal of casting defect calculation.

The reported improvements have been observed in other real case studies for the simulation approaches *P*1, *H*1/*P*8 and *H*-/*P*8 with no opposite results. These dies were designed for engine heads, cylinder blocks, crankcases, pipes and chassis parts. The present research opens new possibilities for using the simulations as design tool in

earlier design phases and for optimization algorithms. Future work will compare other simplification approaches. Searching for simulation reliability and design robustness, the results sensitivity to GDC model parameters will be investigated.

## References

1. Panseri C (1966) Manuale di Fonderia d'Alluminio, 3rd edn. U. Hoepli, Milan
2. Shabani M, Mazahery A (2011) Prediction of mechanical properties of cast A356 alloy as a function of microstructure and cooling rate. Arch Metall Mater 56(3):671–675
3. Flender E, Sturm J (2010) Thirty years of casting process simulation. Int J Metalcast 4(2):7–23
4. Dabade UA, Bhedasgaonkar RC (2013) Casting defect analysis using design of experiments (DoE) and computer aided casting simulation technique. Procedia CIRP 7:616–621
5. Bonazzi E, Colombini E, Panari D, Vergnano A, Leali F, Veronesi P (2017) Numerical simulation and experimental validation of MIG welding of T-joints of thin aluminum plates for top class vehicles. Metall Mater Trans A Phys Metall Mater Sci Volume 48(1):379–388
6. Barral P, Bermúdez A, Muñiz MC, Otero MV, Quintela P, Salgado P (2003) Numerical simulation of some problems related to aluminium casting. J Mater Process Technol 142 (2):383–399
7. Liu B, Xiong S, Xu Q (2007) Study on macro-and micromodeling of the solidification process of aluminum shape casting. Metall Mater Trans B 38(4):525–532
8. Vijayaram TR, Sulaiman S, Hamouda AMS, Ahmad MHM (2006) Numerical simulation of casting solidification in permanent metallic molds. J Mater Process Technol 178(1–3):29–33
9. Vispute P, Chaudhari D (2017) Utilizing flow simulation in the design phase of a casting die to optimize design parameters and defect analysis. Mater Today Proc 4(8):9256–9263
10. Vergnano A, Berselli G, Pellicciari M (2017) Parametric virtual concepts in the early design of mechanical systems: a case study application. Int J Interact Des Manuf 11(2):331–340
11. Prasad D, Ratna S (2018) Decision support systems in the metal casting industry: an academic review of research articles. Mater Today Proc 5(1):1298–1312
12. Anglada E, Meléndez A, Vicario I, Arratibel E, (2015) Cangas. Simplified models for high pressure die casting simulation. Procedia Eng 132:974–98
13. Ilkhchy AF, Jabbari M, Davami P (2012) Effect of pressure on heat transfer coefficient at the metal/mold interface of A356 aluminum alloy. Int Commun Heat Mass Transfer 39(5):705–712
14. Pathak N, Kumar N, Yadav A, Dutta P (2009) Effects of mould filling on evolution of the solid–liquid interface during solidification. Appl Therm Eng 29(17–18):3669–3678
15. Feng H, Chen L, Xie Z, Ding Z, Sun F (2014) Generalized constructal optimization for solidification heat transfer process of slab continuous casting based on heat loss rate. Energy 66:991–998
16. Santos CA, Fortaleza EL, Ferreira CRF, Spim JA, Garcia A (2015) A solidification heat transfer model and a neural network based algorithm applied to the continuous casting of steel billets and blooms. Modell Simul Mater Sci Eng 13:1071–1087
17. Vasileiou AN, Vosniakos GC, Pantelis DI (2017) On the feasibility of determining the heat transfer coefficient in casting simulations by genetic algorithms. Procedia Manuf 11:509–516
18. Zhang L, Li L, Ju H, Zhu B (2010) Inverse identification of interfacial heat transfer coefficient between the casting and metal mold using neural network. Energy Convers Manag 51(10):1898–1904
19. Griffiths WD (1999) The heat-transfer coefficient during the unidirectional solidification of an Al-Si alloy casting. Metall Mater Trans B 30(3):473–482
20. MAGMASOFT®, https://www.magmasoft.de/en/. Accessed on Feb 02 2017